Journal of Advanced Marine Engineering and Technology, Vol. 44, No. 3, pp. 230~235, 2020
J. Advanced Marine Engineering and Technology (JAMET)
https://doi.org/10.5916/jamet.2020.44.3.230

ISSN 2234-7925 (Print)
ISSN 2234-8352 (Online)
Original Paper

Effect of process parameters on coating of a Zn thin film on AZ91D magnesium alloy

Young-Jong Kim†

(Received April 7, 2020 ; Revised May 15, 2020 ; Accepted June 10, 2020)

Abstract: There is an increased interest in the development of lightweight materials with corrosion-resistant coatings in industries such as aerospace, automobile, ship, and electronics. In this study, a Zn thin film is fabricated on a magnesium alloy (AZ91D) substrate by thermo-electron activated ion plating, which is a modified physical vapor deposition (PVD) method that is environmentally friendly and capable of controlling nano-phase particles. The effect of gas pressure and substrate bias voltage on the morphology and crystal orientation of the Zn thin film was analyzed by X-ray diffraction and field emission scanning electron microscopy (SEM). Additionally, the corrosion behavior of the Zn thin film was evaluated by an electrochemical anodic polarization test using a deaerated 3% NaCl solution. All the deposited Zn films showed good corrosion resistance as compared to the bare substrate of AZ91D. It was observed that the morphology of the Zn film was changed from column structure to granular structure by gas pressure. The morphology of the films was affected not only by Ar gas pressure but also by the substrate bias voltage. The effect of increasing bias voltage was similar to reducing gas pressure. Finally, the corrosion resistance of AZ91D was greatly improved by the Zn thin film obtained by optimizing the crystal orientation and the morphology through the plasma ion plating technique.

Keywords: Corrosion resistance, Morphology, Crystal orientation, Ion plating method, Zn thin film, Physical vapor deposit (PVD)

1. Introduction

Globally effort is being made to use new and existing energy resources more economically and efficiently. Magnesium is the lightest metal used in the aerospace, automobile, ship, and electronics industries, and is actively researched for other novel applications **[1]-[5]**. However, the applicability of magnesium is limited due to its vulnerability to environmental corrosion. Surface coating is the most effective way to protect magnesium and its alloys from corrosive environments or to slow down the rate of corrosion **[6]-[12]**. In particular, Zn metal is attracting attention as a coating material for imparting corrosion resistance and improved mechanical properties to magnesium and its alloys **[10]-[12]**. Many studies have been conducted to improve the corrosion resistance of magnesium using wet plating methods such as chromating and anodizing. However, the coatings produced by these methods are uneven, sparse, and not durable enough because of their high defect densities and processing conditions. Moreover, the wet coating process leads to environmental pollution.

In this study, the fabrication of a Zn thin film is attempted by the PVD thermo-electro activated ion plating method, which is a non-polluting plasma membrane processes, to impart corrosion resistance to AZ91D (magnesium alloy). The effect of varying the fabrication conditions such as Ar gas pressure and bias voltage on the morphology and the crystal orientation of the Zn thin film was analyzed from the perspective of Zn diffusion due to the thermal energy. The basic guidelines for conducting the process of Zn coating are presented by examining the effects of the morphology and crystal orientation of the Zn film prepared under these conditions on electrochemical corrosion resistance.

2. Experimental method

Zn thin films were prepared using two types of PVD, called the vacuum deposition and thermo-electro activated ion plating methods. The vacuum deposition method involves evaporation of the raw materials in a vacuum furnace (10^{-3} to 10^{-4} Pa) by resistance heating and deposition on a substrate to produce a thin film. On the other hand, the ion plating method is an improved version of vacuum deposition where the method of

† Corresponding Author (ORCID: https://orcid.org/0000-0002-9772-2899): Ph.D., Division of Marine Engineering, Korea Maritime & Ocean University, 727, Taejong-ro, Yeongdo-gu, Busan 49112, Korea, E-mail: kyjguide@gmail.com, Tel: 051-410-4264

evaporation is the same but the kinetic energy of the evaporated Zn is increased by ionizing the evaporated particles to increase adhesion to the substrate and improve the thin film quality.

Figure 1: Photograph of thermo-electron activated ion plating apparatus

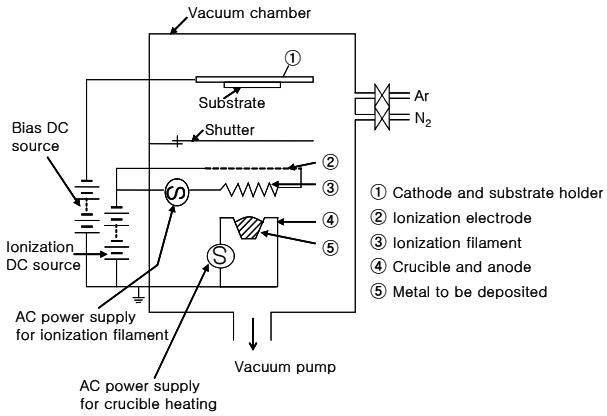

Figure 2: Schematic of the thermo-electron activated ion plating apparatus

Figure 1 and **Figure 2** show a photograph and schematic of the thermo-electro activated ion plating device used in this experiment, respectively. The device is composed of a vacuum source, an evaporation source, an ionization source, and a substrate holder. Zn with a purity of 99.99% was used as the evaporation metal to fabricate the Zn thin film, and magnesium alloy AZ91D was used as the substrate. An ionization filament made of tantalum wire (0.8 mm in diameter) was used to enhance the ionization efficiency. The ionization filament was placed at 4 cm above the evaporator and a negative bias voltage of 150 V with respect to the evaporator and a current of 20 A was supplied to the ionization filament. The source to substrate distance was 13 cm. The Zn thin film was initially fabricated under a vacuum of about 5×10^{-6} Torr, additional samples were prepared by changing the Ar gas pressure and bias voltage conditions. Ar ion-bombardment cleaning was performed before every deposition.

Scanning electron microscopy (SEM, JEOL JSM-5410) was used to observe the surface and cross-sectional morphology of the Zn thin film. The cross-section of the Zn thin film was created by immersing the substrate in liquid nitrogen for about 5 minutes followed by a brittle fracture. The surface and cross-section specimens were sputter-coated with gold to improve the conductivity of the specimen for effective imaging under SEM. The morphology images were captured at an acceleration voltage of 20 kV and different magnifications. In addition, an X-ray diffractometer (XRD, Rigaku Co. D/Max-2000) was used to analyze the crystal orientation of the Zn thin film. The X-ray source for diffraction was Cu Kα, and the voltage and current settings of the X-ray tube were 30 kV and 50 mA, respectively. In addition, Kβ was used as a filter with the scanning speed and the range of 2Θ was 0.05 sec/step and 15° to 75°, respectively. The corrosion resistance for the Zn thin films was evaluated by measuring electrochemical anodic polarization in a de-aerated 3% NaCl solution. The CMS 100 corrosion test system from Gamry (USA) was used as a potentiostat to perform the polarization measurements. The voltage measurement was referenced against the silver/silver chloride electrode with a scanning speed of 2 mV/sec. A voltage range of 0 to 2 V was used based on the open circuit potential. The surface area of the specimen exposed to the solution was kept at 1.0×1.0 cm^2 and the remaining specimen was insulated with epoxy resin.

3. Results and Discussion

3.1 Crystal orientation and morphology of Zn thin film

The physical and chemical properties of the evaporated metal films depend on the crystal orientation and morphology of the films, which is influenced by the deposition conditions **[13]-[20]**. Therefore, it is important to capture the changes in crystal orientation and morphology of the film due to changes in deposition conditions to improve the corrosion resistance of Zn thin films. To investigate the effect of crystal orientation due to changes in the vacuum level, the Zn thin film prepared by changing only the Ar gas pressure at each bias voltage was analyzed by XRD. The relative intensities of the X-ray diffraction peaks are shown in **Figure 3**.

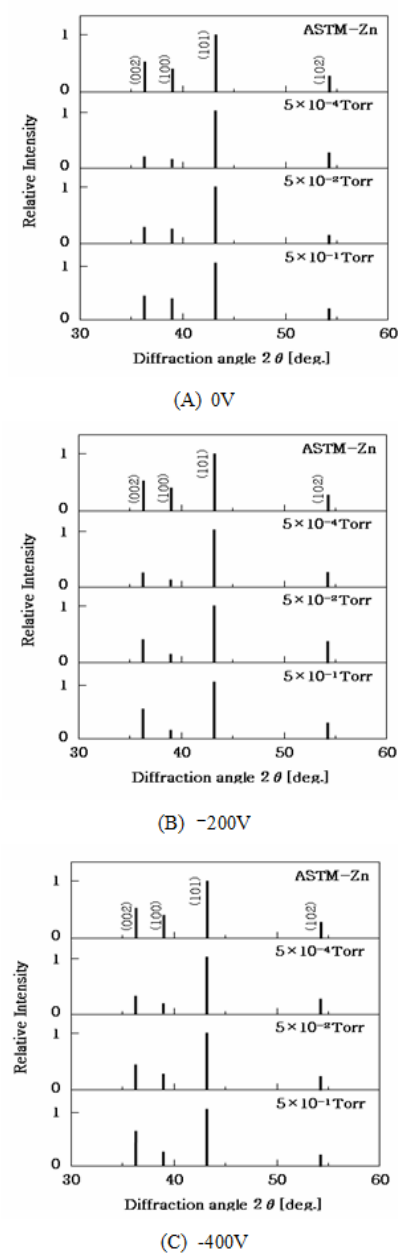

Figure 3: X-ray diffraction patterns of Zn films deposited at various bias voltages

At a vacuum of 5×10^{-4} Torr, a small amount of residual Ar gas is present. Whereas, at 5×10^{-2} Torr gases like oxygen, nitrogen, and water are also present along with Ar in the vacuum chamber. These gases adsorb strongly on the (002) face which has a high surface energy, therefore the crystal growth caused by the deposition of particles can be hindered, and thus the growth rate would be slower than that of the (101) face having relatively low surface energy.

As a result, the area occupancy of a surface having high surface energy would become high. **Figure 3** shows that when the Ar gas pressure was 5×10^{-1} Torr, the strength of the (002) face increased significantly compared to the (101) face, as compared to that at 5×10^{-4} Torr and 5×10^{-2} Torr. This could be the result of preferential adsorption of the residual gas on (002) face, which has high surface energy. In other words, the adsorption of residual Ar gas on the crystal nucleus would lead to the formation of multiple nuclei rather than continuous growth. As a result, the morphology of the film is expected to be particulate in nature.

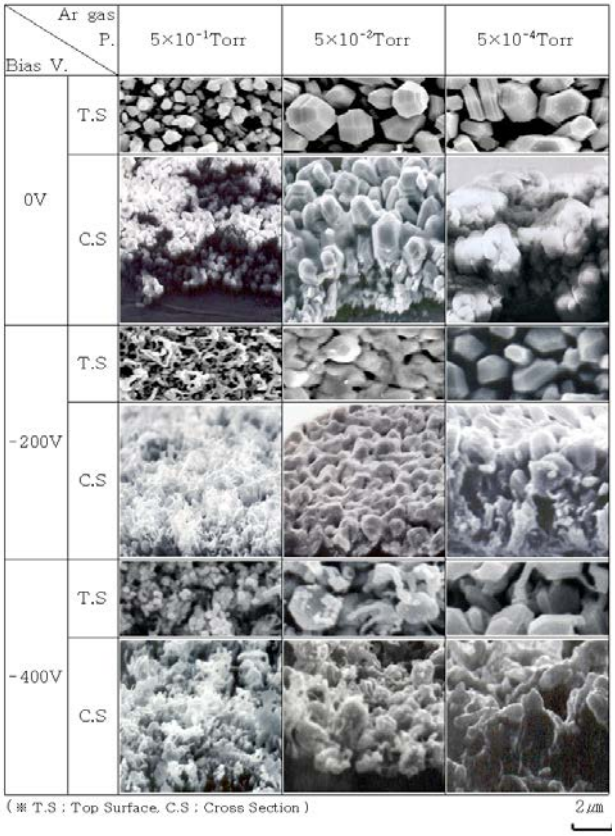

Figure 4: SEM photographs of Zn films deposited at different Ar gas pressures

Next, the effect of bias voltage on crystal structure is analyzed. As shown in **Figure 3**, the ratio of the intensity of (002) face to that of (101) face increases when the bias voltage is decreased from 0 V to -200 V. However, when the pressure increases to 5×10^{-1} Torr, the effect of adsorption of Ar gas on the film deposition dominates in comparison to the bias voltage. This could be due to the increased availability of Ar gas for adsorption from all sides. In particular, the high affinity of Ar gas towards (002) face leads to a surface dominated by (002) orientation. **Figure 4** shows SEM images of the morphology of the top surface and cross-section of Zn thin films prepared by increasing the Ar gas pressure while keeping the bias voltage

constant. When the bias voltage is 0 V, as the Ar gas pressure increases some defects are observed in the crystal grains and the size of the grains on the top surface and the cross-section become small. Also, a decrease in the Zn film thickness is observed as the gas pressure increases. When the bias voltage is reduced to -200 V, the size of the crystal grains on the top surface becomes fine while that on the cross-section becomes small and dense. A similar trend in the morphology is observed when the bias voltage is further reduced to -400 V.

Now we analyze the results of morphology in relation to the X-ray diffraction results shown in **Figure 3** to examine the process of thin-film formation. When the Ar gas pressure is high (in the case of low vacuum - 5×10^{-1} Torr), Volmer-Weber growth occurs in a direction perpendicular to the substrate, such as the (101) face, where the surface energy is relatively lower than the (002) face. Also, the growth is suppressed on (002) face due to the residual gas in the vacuum container. When the bias voltage is increased in the negative direction, the atom transfer effect, heating effect, and the sputtering effect increases causing the adsorbent atom to desorb from the growth surface on the substrate. Here, an increase in the atomic mobility facilitates surface diffusion. Therefore, as the bias voltage is increased in the negative direction, the Zn atoms diffuse to the film formation surface, so the crystal grains on the surface become large and the width of the columnar structure becomes thick. As the bias voltage is increased, the sputtering effect, the moving effect, and the heating effect are also increased by the ionized and activated Ar gas, which leads to a thick columnar cross-section. In the case of the Ar gas pressure of 5×10^{-1} Torr, the surface free energy of Zn particles is reduced due to the presence of Ar gas and columnar crystal growth is suppressed. Thus, as the nuclear growth is suppressed the crystal grains on the surface are small and the cross-section has a granular crystal structure.

3.2 electrochemical corrosion resistance of Zn thin film

Figure 5 shows the results of the electrochemical anodic polarization measurement of Zn thin films in a deaerated 3% NaCl solution. In the case of the bias voltage of 0 V, the Zn thin film specimen prepared under Ar gas pressure of 5×10^{-1} Torr showed better corrosion resistance than the 99.99% Zn-ingot and AZ91D.

Additionally, as the gas pressure increased the corrosion resistance of the Zn thin film improved on account of low passivation current density. When the bias voltage was -200 V, the Zn thin film prepared under all gas pressure conditions showed better corrosion resistance than both the 99.99% Zn-ingot and AZ91D sample.

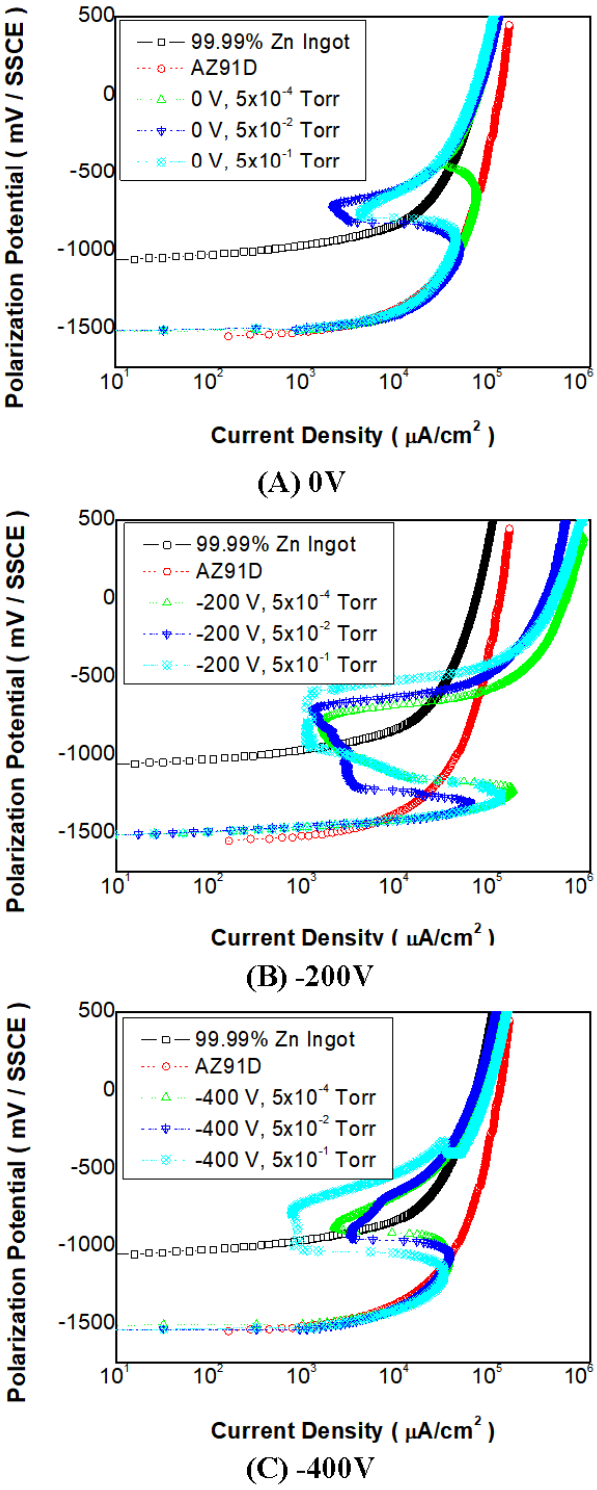

Figure 5: Anodic polarization curves of Zn films deposited at various bias voltages measured in deaerated 3% NaCl solution

In addition, the corrosion resistance improved as the gas pressure increased, similar to the case where the bias voltage is

0 V. The best corrosion resistance was observed when the bias voltage is -200 V and the Ar gas pressure was 5×10^{-1} Torr. Even under the bias voltage of -400 V, the Zn thin film showed good corrosion resistance as compared to the 99.99% Zn-ingot and AZ91D sample.

The corrosion behavior of the Zn thin film is analyzed in relation to the morphology and crystal orientation of the top surface and cross-section. As observed in the SEM images, the size of the grains of the top surface of the Zn film as well as the cross-section decreased as the Ar gas pressure increased. The fact that the grain size of the top surface is small means that the area occupied by the grain boundary on the top surface is large. It is well-known that the grain boundary acts as an anode because it is regarded as a kind of defect. In the case of a Zn film having a relatively large area occupied by the grain boundary, the grain boundary acts as an active anode in the environment. This is similar to the formation of an oxide film on the surface of the aluminum. Moreover, when the grain boundary is small and the area occupied by the grain boundary is large, a dense passivation oxide film forms relatively quickly. When the passivation film is formed on the grain boundary as described above, the film on the orientation face having a higher surface energy than that of the (101) face and the (002) face acts as a grain boundary to promote the formation of the passivation film. This is an active form because the face having lower surface energy is chemically unstable. In other words, the Zn thin film with a small crystal grain on the surface and oriented toward the (002) face is excellent for corrosion resistance because it makes a dense passivation film in a deaerated 3% NaCl solution. In addition, when pitting corrosion occurs, the granular structure with fewer defects than the columnar structure is expected to have a small dissolution rate. This is because the area of the granular structure exposed to the solution is smaller than the columnar structure morphology.

4. Conclusion

As the gas pressure increased, the crystals of the Zn thin film were first oriented, showing a relatively high X-ray diffraction peak on the face with a high surface energy compared to the plane with a low surface energy. This is presumably caused by the relative increase in the area occupied on the plane with inhibition of the growth of crystal nuclei. This is because the gas with the higher surface energy was adsorbed earlier than the plane with a high surface energy with increasing gas pressure. The Zn thin film prepared in this study showed better corrosion resistance than the 99.99% Zn-ingot. In addition, the more the crystal grains changed to a small-grained crystal structure, the lower was the passive current and the more positive was the direction of the pitting corrosion potential. As the Ar gas pressure increased, the crystal grains decreased in size, and the cross section changed from a columnar structure to granular structure. The crystal orientation and morphology control of this study were successfully demonstrated to increase the corrosion resistance of a Zn thin film.

Author Contributions

Conceptualization, Y. J. Kim; methodology, Y. J. Kim; Software, Y. J. Kim; Formal Analysis, Y. J. Kim; Investigation, Y. J. Kim; Resources, Y. J. Kim; Data curation Y. J. Kim; Writing-Original Draft Preparation, Y. J. Kim; Writing-Review & Editing, Y. J. Kim; Visualization, Y. J. Kim; Supervision, Y. J. Kim; Project Administration, Y. J. Kim; Funding Acquisition, Y. J. Kim.

References

[1] Y. S. Yun, “A study on the surface treatment of magnesium for marine engine systems,” Journal of the Korean Society of Marine Engineering, vol. 35, no. 2, pp. 252-257, 2011 (in Korean).

[2] J. D. Kim, B. L. Kil, and J. H. Lee, “Effect of process parameters on laser weldability of AZ31 magnesium alloy,” Journal of the Korean Society of Marine Engineering, vol. 32, no. 4, pp. 570-577, 2008 (in Korean).

[3] X. Zhan, W. Shang, Y. Wen, Y. Li, and M. Ma, “Preparation and corrosion resistance of a three-layer composite coatings on the Mg alloy,” Journal of Alloys and Compounds, vol. 774, pp. 522-531, 2019.

[4] Y. Wang, Z. Gu, J. Liu, J. Jiang, N. Yuan, J. Pu, and J. Ding, “An organic/inorganic composite multi-layer coating to improve the corrosion resistance of AZ31B Mg alloy,” Surface and Coatings Technology, vol. 360, pp. 276-284, 2019.

[5] R. C. Zeng, Y. Hu, F. Zhang, Y. D. Huang, Z. L. Wang, S. Q. Li, and E. H. Han, “Corrosion resistance of cerium-doped zinc calcium phosphate chemical conversion coatings on AZ31 magnesium alloy,” Transaction of Nonferrous Metals Society of China, vol. 26, no. 2, pp. 472-483, 2016.

[6] N. V. Phuong, M. Gupta, and S. Moon, “Enhanced corrosion performance of magnesium phosphate conversion coating on AZ31 magnesium alloy,” Transaction of Nonferrous Metals Society of China, vol. 27, no. 5 pp. 1087-1095, 2017.

[7] X. B. Chen, M. A. Easton, N. Birbilis, H. Y. Yang, and T. B. Abbott, “Corrosion-resistance coating for magnesium (Mg) alloys,” Corrosion Prevention of Magnesium Alloys, pp. 282-312, 2013.

[8] S. Bender, J. Göllner, A. Heyn, C. Blawert, and P. Balasrinivasan, “Corrosion and surface finishing of magnesium and its alloys,” Fundamentals of Magnesium Alloy Metallurgy, pp. 232-265, 2013.

[9] S. Akavipat, E. B. Hale, C. E. Habermann, and P. L. Hagans, “Effects of iron implantation on the aqueous corrosion of magnesium,” Materials Science and Engineering, vol. 69, no. 2, pp. 311-316, 1985.

[10] X. Wang, X. Wang, D. Wang, M. Zhao, and F. Han, “A novel approach to fabricate Zn coating on Mg foam through a modified thermal evaporation technique, Journal of Materials Science & Technology, vol. 34, no. 9, pp. 1558-1563, 2018.

[11] A. Bordbar-Khiabani, B. Yarmand, and M. Mozafari, “Enhanced corrosion resistance and in-vitro biodegradation of plasma electrolytic oxidation coatings prepared on AZ91 Mg alloy using ZnO nanoparticles-incorporated electrolyte,” Surface and Coatings Technology, vol. 360, pp. 153-171, 2019.

[12] C. Zhao, H. Wu, P. Hou, J. Ni, P. Han, and X. Zhang, “Enhanced corrosion resistance and antibacterial property of Zn doped DCPD coating on biodegradable Mg,” Materials Letters, vol. 180, pp. 42-46, 2016.

[13] M. J. Brett, “Structural transitions in ballistic aggregation simulation of thin-film growth,” Journal of Vacuum Science & Technology A, vol. 6, no. 3, pp. 1749-1751, 1988.

[14] J. A. Thornton, “Influence of apparatus geometry and deposition conditions on the structure and topography of thick sputtered coatings,” Journal of Vacuum Science & Technology, vol. 11, no. 4, pp. 666-670, 1974.

[15] M. H. Lee, Y. Hasegawa, and T. Oki, “Preparation of Al thin films by thermo-electron activation ion plating and their corrosion resistance,” Journal of The Japan Institute of Metals, Nippon Kinzoku Gakkaishi, vol. 57, no. 6, pp. 686-691, 1993.

[16] J. A. Thornton, “High rate thick film growth,” Annual Review of Materials Science, vol. 7, no. 1, pp. 239-260, 1977.

[17] R. Messier, A. P. Giri, and R. A. Roy, “Revised structure zone model for thin film physical structure,” Journal of Vacuum Science & Technology A: Vacuum, Surfaces, and Films, vol. 2, no. 2, pp. 500-503, 1984.

[18] R. Messier, “Toward quantification of thin film morphology,” Journal of Vacuum Science & Technology A, vol. 4, no. 3, pp. 490-495, 1986.

[19] L. Hultman, J. E. Sundgren, L. C. Markert, and J. E. Greene, “Ar and excess N incorporation in epitaxial TiN films grown by reactive bias sputtering in mixed Ar/N_2 and pure N_2 discharges,” Journal of Vacuum Science & Technology A, vol. 7, no. 3, pp. 1187-1193, 1989.

[20] A. G. Dirks and H. J. Leamy, “Columnar microstructure in vapor-deposited thin films,” Thin Solid Films, vol. 47, no. 3, pp. 219-233, 1977.